Journal of General Virology (1999), **80**, 2889–2900. Printed in Great Britain

Human herpesvirus-8-encoded LNA-1 accumulates in heterochromatin-associated nuclear bodies

Laszlo Szekely,[1] Csaba Kiss,[1] Karin Mattsson,[1] Elena Kashuba,[1] Katja Pokrovskaja,[1] Attila Juhasz,[2] Pia Holmvall[1] and George Klein[1]

[1] Microbiology and Tumor Biology Center, Karolinska Institute, S171 77, Stockholm, Sweden

[2] Department of Microbiology, University Medical School of Debrecen, H-4012 Debrecen, Hungary

Subnuclear distribution of the human herpesvirus-8 (HHV-8)-encoded nuclear protein LNA-1 was analysed at high resolution in body cavity (BC) lymphoma-derived cell lines, in cell hybrids between BC cells and various human and mouse cells and in freshly infected K562 and ECV cell lines. Three-dimensional reconstruction of nuclei from optical sections and quantitative analysis of the distribution of LNA-1 fluorescence in relation to chromatin showed that LNA-1 associates preferentially with the border of heterochromatin in the interphase nuclei. This was further confirmed in the following systems: in endo- and exonuclease-digested nuclei, in human–mouse (BC-1–Sp2-0) hybrids and on chromatin spreads. LNA-1 was found to bind to mitotic chromosomes at random. Epstein–Barr virus (EBV), but not HHV-8, was rapidly lost from mouse–human hybrid cells in parallel with the loss of human chromosomes. HHV-8 could persist on the residual mouse background for more than 8 months. In early human–mouse hybrids that contain a single fused nucleus, LNA-1 preferentially associates with human chromatin. After the gradual loss of the human chromosomes, LNA-1 becomes associated with the murine pericentromeric heterochromatin. In human–human hybrids derived from the fusion of the HHV-8-carrying BCBL-1 cells and the EBV-immortalized lymphoblastoid cell line IB4, LNA-1 did not co-localize with EBNA-1, EBNA-2, EBNA-5 or EBNA-6. LNA-1 was not associated with PML containing ND10 bodies either. DNase but not RNase or detergent treatment of isolated nuclei destroys LNA-1 bodies. In advanced apoptotic cells LNA-1 bodies remain intact but are not included in the apoptotic bodies themselves.

Introduction

Human herpesvirus-8 (HHV-8) is a close relative of herpesvirus saimiri (Neipel *et al.*, 1998) and a more distant relative of Epstein–Barr virus (EBV). HHV-8 causes predominantly asymptomatic infections. The frequency of seropositives varies greatly between different geographical locations, $< 10\%$ in USA and Western Europe (Zong *et al.*, 1997; Martin *et al.*, 1998) and $> 40\%$ in sub-Saharan Africa (He *et al.*, 1998; Mayama *et al.*, 1998), although the exact prevalence has not been established (Rabkin *et al.*, 1998).

HHV-8 is uniformly present in all forms of Kaposi's sarcoma (KS) including classic, endemic, AIDS-associated and post-transplant KS and is thought to contribute to the malignant transformation (Knowles *et al.*, 1997; Kennedy *et al.*, 1998). HHV-8 can immortalize primary endothelial cells (Flore *et al.*, 1998). It is also present in $CD19^+$ peripheral B-cells of KS patients.

Although HHV-8 was not found to transform B-cells *in vitro*, double infection together with EBV generated immortalized lymphoblastoid cell lines (LCLs) that carried both viruses (Kliche *et al.*, 1998). HHV-8 is also present in body cavity (BC) lymphomas and in multicentric Castleman's disease, suggesting that the virus may play an aetiological role in these diseases.

HHV-8 contains at least 14 genes that are very similar to cellular genes (Nicholas *et al.*, 1998; Whitby *et al.*, 1998). Some of them, such as the orf72-encoded v-cyclin, are mainly expressed during the latent phase of the infection and are important candidates for the putative transforming function of HHV-8 (for reviews see Moore *et al.*, 1998; Weiss *et al.*, 1998).

The major latency-associated nuclear antigen (LNA-1) has no cellular homologue. It shows no sequence similarity to any of the EBV-encoded nuclear antigens either. It is encoded by orf73 and transcribed as part of a polycistronic message. It migrates on SDS–polyacrylamide gels with an apparent

Author for correspondence: Laszlo Szekely.
Fax +46 8 330498. e-mail lassze@ki.se

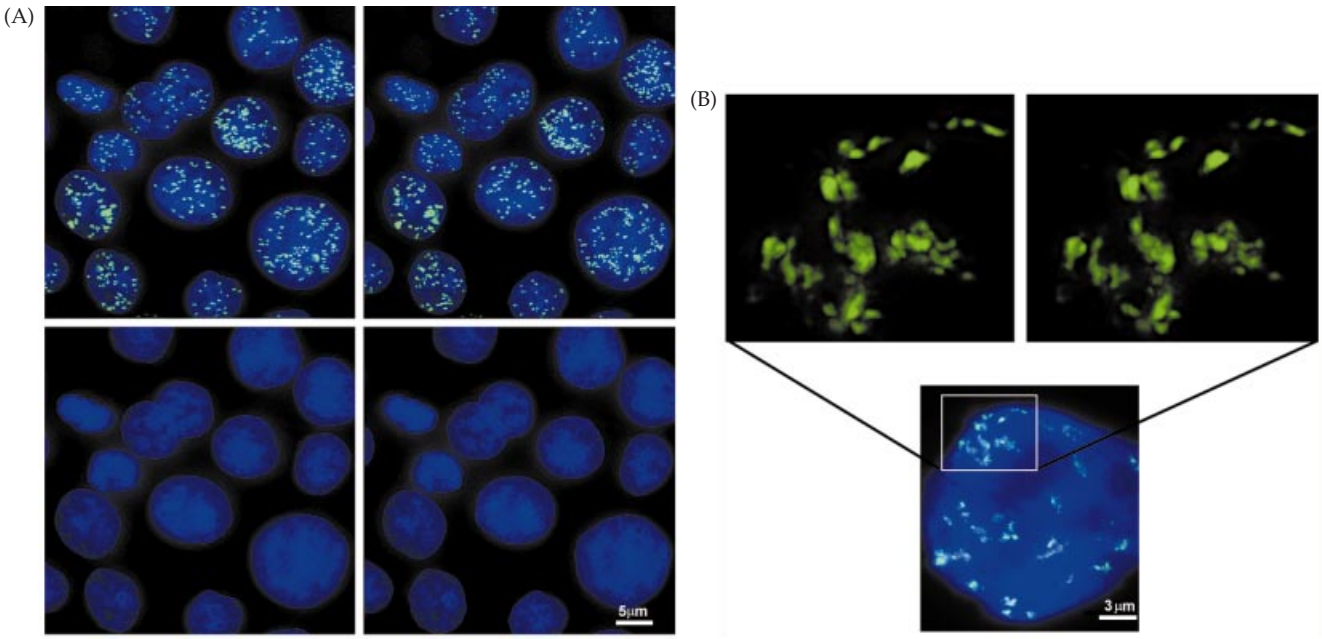

Fig. 1. (A) Stereo image of a group of BCBL-1 nuclei with LNA-1 bodies of varying numbers and size. Comparison of three-dimensional distribution of areas with different DNA content (bottom stereo pair, blue) with the three-dimensional projected distribution of LNA-1 bodies on the DNA background (top stereo pair, green and blue respectively) suggests that the LNA-1 bodies preferentially associate with the heterochromatin borders. (B) Reconstitution of a BCBL-1 nucleus stained for LNA-1 (green) and DNA (blue) from a series of deblurred optical sections at high magnification. Stereoimage projection of the magnified block shows the three-dimensional reconstituted structure of a cluster of irregularly shaped, branching LNA-1 bodies.

mobility of 226–234 kDa. KS patients regularly have very high antibody titres against LNA-1. The antibodies are directed against the immunodominant epitopes located at the C terminus (Kedes *et al.*, 1997; Rainbow *et al.*, 1997; Boshoff *et al.*, 1998; Dittmer *et al.*, 1998; Sarid *et al.*, 1998).

LNA-1 accumulates in nuclear bodies in interphase nuclei, producing a characteristic stippled pattern. We have shown that LNA-1 bodies remain associated with the mitotic chromosomes. They did not co-localize with EBNA-1 in the doubly infected BC lymphoma line BC-1 (Szekely *et al.*, 1998).

In the present study we have investigated the high resolution intranuclear distribution of LNA-1 in relation to the chromatin and known nuclear structures in BC cells, cell hybrids and freshly infected cells.

Methods

■ **Cell culture and virus production.** All cell lines were cultured at 37 °C, in Iscove's medium containing 10% foetal calf serum and 50 mg/ml gentamycin. The absence of mycoplasma contamination was monitored by periodic staining with Hoechst 33258. The following lines were used in this study: human body cavity lymphoma lines BC-1 and BCBL-1, IB4 and CBM1-Ral-Sto EBV-immortalized LCLs, the human endothelial line ECV, the erythroleukaemia line K562, the colon carcinoma line SW480, the CV-1 kidney epithelial line, the Sp2-0 mouse myeloma line and NIH3T3 mouse fibroblasts.

HHV-8 was produced by treating BCBL-1 cells with 20 ng/ml TPA for 7 days. The cell-free supernatant was filtered through a 0·45 μm filter and used in a dilution of 1:5 to infect the target cells for 48 h.

■ **Visualization of heterochromatin by endonuclease treatment and chromatin spreading.** Mechanical spreading of unfixed nuclei was done as previously described (Szekely *et al.*, 1996). To visualize heterochromatin by endonuclease digestion, methanol–acetone fixed cells were digested with *Sau*3A restriction enzyme in 20 mM Tris–HCl pH 7·5, 7 mM $MgCl_2$, 100 mM KCl, 2 mM β-mercaptoethanol for 2 h at 37 °C using a fivefold dilution series of the enzyme. Slides showing a high contrast between loose and compact chromatin on Hoechst 33258 staining were used for detailed analysis.

■ **DNase and RNase treatment of isolated nuclei.** BCBL-1 cells were treated with ice-cold nucleus isolation buffer containing 50 % glycerol, 10 mM Tris–HCl, pH 7·5, 10 mM NaF, 1 mM EDTA and 0·1% NP40 for 10 min. For hypotonic lysis the glycerol concentration was decreased to 10%. The single cell suspension was passed through 25 ***g*** twice, pelleted for 5 min at 1000 ***g*** and the nuclei were resuspended in isolation buffer supplemented with 10 mM Mg_2-acetate. The isolated nuclei were digested at 37 °C for 30 min with 0·5 mg/ml DNase I or 0·5 mg/ml RNase or with both. The digested nuclei were centrifuged on glass slides in Cytospin, fixed with methanol–acetone and stained for LNA-1.

■ **Production of cell hybrids.** HHV-8-carrying BC-1 and BCBL-1 cells were fused with the mouse plasmacytoma cell line Sp2-0 or with EBV-carrying IB4 cells using a modified hybridoma protocol. Briefly the cells were washed with serum-free Iscove's medium, mixed with each other. After centrifugation for 5 min at 1200 ***g*** the pellet was exposed to 50% PEG 1500, 5% DMSO, 45% Iscove's medium and preheated to 37 °C for 60 s with constant stirring. The fusion mixture was gradually diluted to 10 ml with Iscove's medium during the following 2 min, centrifuged for 5 min at 1200 ***g*** and resuspended in Iscove's medium containing 10% foetal calf serum. To select stable mouse–human hybrids of the $HGPRT^-$ Sp2-0 and the ouabain-sensitive BCBL-1 cells, the

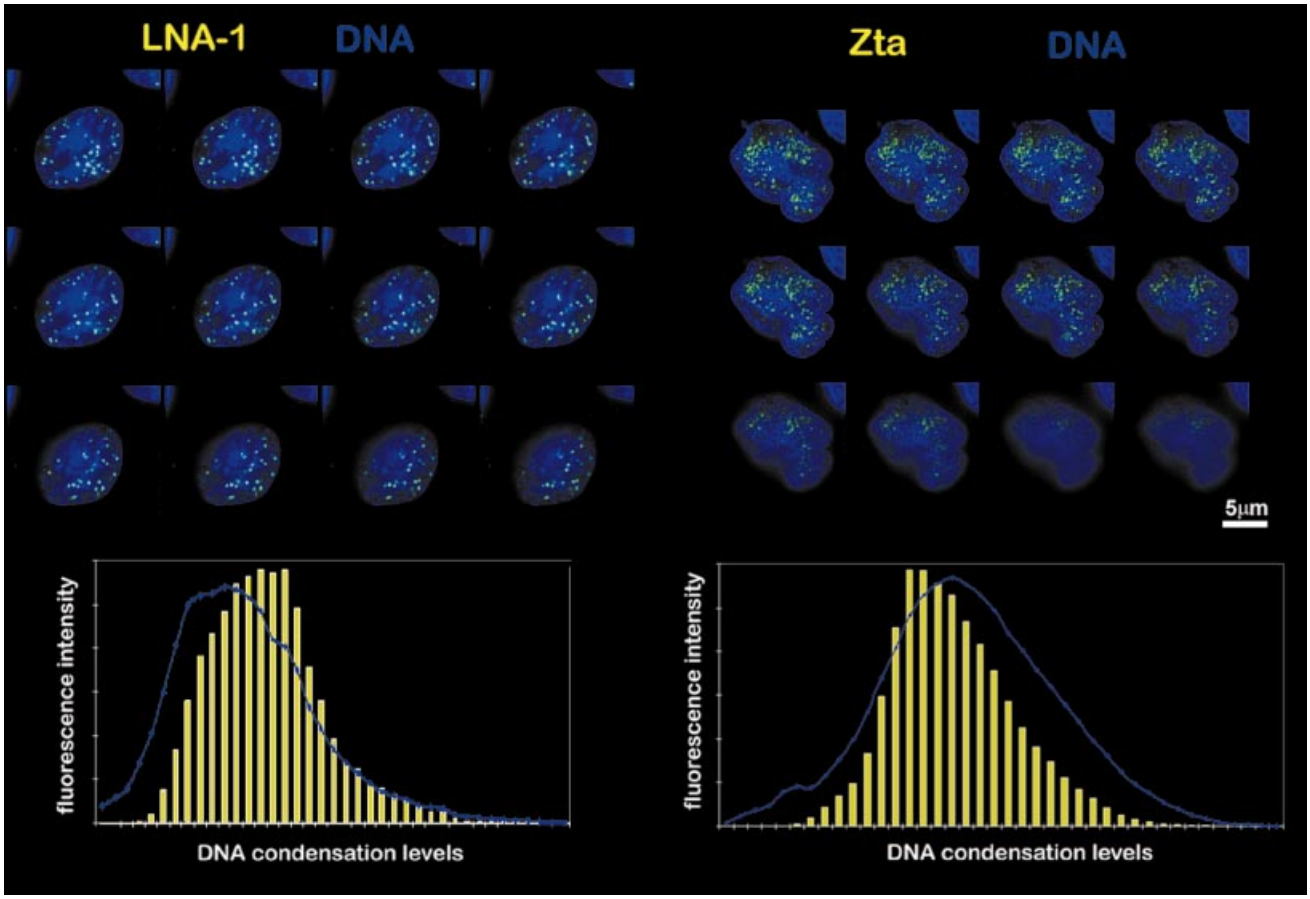

Fig. 2. Quantitative comparison of fluorescent intensity distribution of nuclear proteins (LNA-1 or Zta, green) and DNA (blue) as a function of the intensity of the underlying DNA staining. A BCBL-1 (left panel) and a B95-8 (right panel) nucleus were optically sectioned, deblurred and the sections were arranged as a mosaic image. Intensity distribution of DNA staining was normalized to 4096 grey scale levels and the scale was divided into forty consecutive intensity levels (*x* axis). Pixels corresponding to the individual intensity levels were identified and their summarized green and blue intensities values were calculated (*y* axis) producing intensity distribution charts for the nuclear proteins (yellow columns) and DNA (blue curves). The distribution of LNA-1 showed a right shift in relation to the intensity distribution of DNA, whereas Zta always showed a left shift, indicating that they localize to high and low DNA density areas respectively.

medium was supplemented with 5×10^{-4} M ouabain (Sigma) and 1 × hypoxanthine–aminopterin–thymidine (HAT) selection mixture.

■ **Immunofluorescence staining and image analysis.** Sera with high anti-LNA-1 titres were collected from patients suffering from the classical form of KS at the Dermatology Unit of Debrecen Medical School, Hungary, and stored at −20 °C.

The cells were regularly fixed with methanol–acetone (1:1) at room temperature for at least 10 min and rehydrated in PBS. Sera were diluted in blocking buffer (2% BSA, 0·2% Tween-20, 10% glycerol, 0·05% NaN_3 in PBS). The first antibody was incubated with the cells for 30 min at room temperature followed by three 2 min washes in PBS. The secondary, fluorochrome-conjugated antibody was diluted in blocking buffer (1:20) and incubated with the cells for an additional 30 min. Following four PBS washes the slides were mounted with 70% glycerol containing 2·5% DABCO (Sigma) anti-fading agent.

Double immunofluorescence staining for PML, Sp100, EBNA-1, EBNA-2, EBNA-5, EBNA-6, LMP-1 and LNA-1 was carried out as described (Szekely *et al.*, 1995, 1996, 1998; Pokrovskaja *et al.*, 1997).

The images were produced using a Leitz DM RB microscope, equipped with Leica PL Fluotar 100 ×, 40 × and PL APO Ph 63 × oil immersion objectives. Leica L4, Tx and A composite filter cubes were used for the FITC, Texas red and Hoechst 33258 fluorescence respectively. The pictures were captured with a Hamamatsu dual mode cooled CCD camera (C4880) and recorded and analysed on a Pentium PC computer equipped with an AFG VISION*plus*-AT frame grabber board using Hipic3.2.0 (Hamamatsu), Image-Pro Plus (Media Cybernetics) and Adobe Photoshop image capturing and processing software.

■ **Three-dimensional microscopy and image quantification.** Images were acquired by a Zeiss Axiophot microscope, equipped with 16 × oil Plan-Neofluar NA 0·5, 63 × oil Plan-Apochromat NA 1·4 and 100 × oil Plan-Neofluar NA 0·7–1·3 objectives, illuminated with Osram HBO 100 W mercury short arc lamp. The following excitation filters, mounted in the computer-controlled filter wheel were used: single band UV exciter for Hoechst (84360), single band blue exciter for FITC (84490), single band green exciter for TRITC (84555). The emission filter was a multiple band pass filter (84000) mounted on a static stage. All filters were from Chroma Technology. The filter wheel, dual shutter and Z axis motor were controlled through a LEP MAC2000 Communication Interface 73000400 using RS-232 serial connection (from Ludl Electric Products, Hawthorne, NY, USA). Images were captured with a PXL

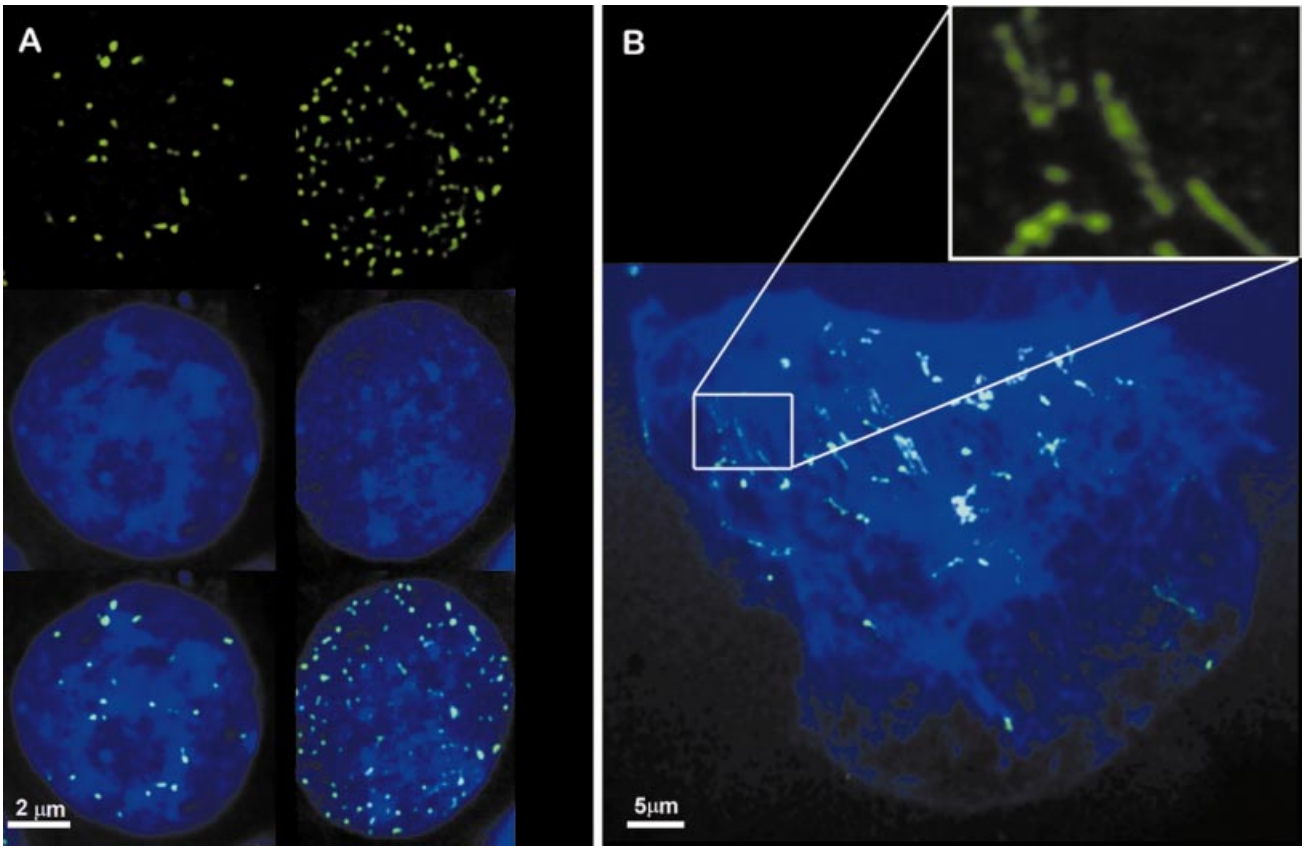

Fig. 3. (A) Association with heterochromatin is independent of the number of LNA-1 bodies (≈ 25 left nucleus, ≈ 124 right nucleus) in BCBL-1 nuclei. *Sau*3A digestion was used to increase the staining difference between euchromatin and heterochromatin. LNA-1 staining (top), *Sau*3A-digested DNA (middle) and their superposition (bottom). (B) Unlike nuclear bodies associated with the nucleoskeleton, LNA-1 bodies are not resistant to mechanical spreading but stretch together with the outpouring DNA.

cooled CCD camera (Photometrix) operating at −25 °C, using 12 bit (4096 grey scale level) capture mode. The hardware control and image processing was provided by an Indy Silicon Graphics computer equipped with a MIPS R4600 CPU and a MIPS R4610 floating point processor. The operation system was IRIX 5.3. The imaging programs were written and operated using the Isee 3.4 graphical programming system (Inovision) as described (Holmvall *et al.*, 1999).

■ **GFP–LNA-1-C′ fusion construct.** A 418 nucleotide long fragment covering the coding region aa 939–1121 was PCR-amplified from BCBL-1 cells using the primers: 5′ GAGGATCCGAATACCGCTATGTA-CTCAG 3′ and 5′ CTGAATTCCTAGGCGGGCCATTTGTACT 3′. The fragment was subcloned into the GST-2TK vector (Pharmacia), sequenced and further subcloned into the pEGFP vector (Clontech). The GFP–LNA-1-C′ plasmid was transfected into CV-1 cells as described.

■ **Detection of EBV and HHV-8 by PCR.** PCR amplification of genomic fragments of EBV and HHV-8 was done in glass capillaries using Rapid Cycler (Idaho Technologies). The reactions were carried out in 10 μl vol. using 2 mM $MgCl_2$, 1 μM primer and 200 μM dNTP mixture and 0·1 U Platinum Taq polymerase. The initial 15 s denaturation at 94 °C was followed by 35 cycles of denaturation at 94 °C for 0 s, annealing at 50 °C for 0 s and elongation at 72 °C for 45 s. The primer pair for EBV was 5′ CTAGGCCACCTTCTCAGT 3′ and 5′ CTTCT-CTGCTCGTTACCA 3′, which amplifies a 1087 bp long fragment from the W-repeats. The LNA-1 C terminus primers were used to detect HHV-8.

Results

Association of LNA-1 bodies with heterochromatin in human cells

BC-1 or BCBL-1 cell populations show considerable variation in the number (between ∼ 10 and ∼ 200), size and staining intensity of LNA-1 bodies. To generate microscopic images of LNA-1 bodies that are free of out-of-focus blur, represent all the relevant focal planes, and preserve depth information, we used three-dimensional computer-controlled wide-field epifluorescence microscopy with automatic deblurring. Microscopic analysis of many BCBL-1 nuclei suggested that the LNA-1 bodies are not randomly distributed in relation to the chromatin but preferentially associate with the border of heterochromatin (Fig. 1A). Three-dimensional reconstitution of BCBL-1 nuclei shows that the bodies do not have a uniform morphology. They often form small local clusters of irregularly shaped branching subunits (Fig. 1B).

For further analysis we applied a new computer program that we have developed that quantifies the fluorescent signal from a deconvoluted series of focal sections of a single nucleus in relation to forty different intensity levels of the cor-

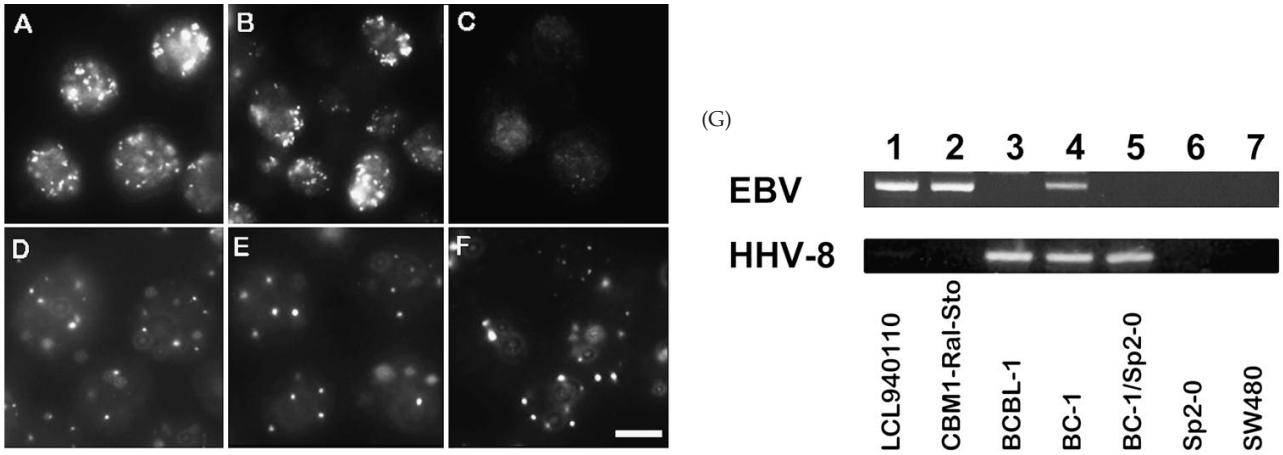

Fig. 4. (A–F) LNA-1 bodies persist in isolated nuclei released by hypotonic lysis in the presence of detergent (A), are not effected by subsequent treatment with RNase (B), but are destroyed by DNase I treatment (C). Nucleoskeleton-associated PML bodies (ND10) are resistant to all of these treatments (D, E, F respectively). (G) Persistence of HHV-8 and elimination of EBV DNA from BC-1–Sp2-0 hybrids 2 months after fusion as detected by PCR of the EBV W repeat and the orf73 of HHV-8. Lanes 1, LCL940110$^{(EBV+/HHV-8-)}$; 2, CBM1-Ral-Sto$^{(+/-)}$; 3, BCBL-1$^{(-/+)}$; 4, BC-1$^{(+/+)}$; 5, BC-1–Sp2-0 hybrid$^{(-/+)}$; 6, Sp2-0$^{(-/-)}$; 7, SW480$^{(-/-)}$.

responding focal planes stained for DNA by Hoechst 33258 (Holmvall *et al.*, 1999). Plotting the distribution of LNA-1 staining intensity as a function of the corresponding DNA condensation levels, in comparison with the intensity distribution of the DNA itself showed shifts to the right in all 16 analysed nuclei. This indicates that LNA-1 staining was preferentially associated with the high DNA density areas. A similar analysis of the EBV-encoded nuclear EBNA-2 and Zta-1 proteins showed an opposite shift to the left, indicating that these proteins were primarily located in the low DNA density areas (Fig. 2).

LNA-1 bodies in endonuclease-treated or mechanically spread cells

To facilitate the direct visualization of the heterochromatin association of LNA-1, cytospin smears of BC-1 and BCBL-1 cells were treated with the frequently cutting restriction endonuclease *Sau*3A. This treatment decreases the staining intensity of euchromatin but has no effect on the more condensed heterochromatin. Under these conditions the LNA-1 bodies were preferentially associated with the borders of the compacted chromatin but were not inside them (Fig. 3A).

Mechanical spreading of living BCBL-1 cells, followed by fixation and immunostaining, further confirmed the association with the condensed chromatin. It also showed that the LNA-1 bodies are not rigid structures but extend in parallel with the stretching chromatin (Fig. 3B).

LNA-1 in DNase-, RNase- and detergent-treated nuclei

In order to study the association of LNA-1 with DNA, RNA or nucleoskeleton, BCBL-1 nuclei were isolated by hypotonic or isotonic lysis in the presence of a non-ionic detergent. Neither the nucleus isolation nor the subsequent treatment with RNase had any effect on LNA-1 staining. In contrast, digestion of isolated nuclei with DNase I almost completely eliminated the LNA-1 staining while neither DNase nor RNase treatment affected the staining of nucleoskeleton-associated PML bodies (Fig. 4A–F).

LNA-1 in human–mouse hybrids

In contrast to human cells where the border between euchromatin and heterochromatin is not very clear, mouse cell nuclei are characterized by pericentromeric heterochromatin appearing in the form of well defined chromatin blobs with a high concentration of DNA. In order to study the distribution of LNA-1 in relation to mouse heterochromatin we generated cell hybrids between the ouabain-sensitive BC-1 and BCBL-1 cells and the HGPRT^{-} Sp2-0 mouse myeloma line, the universal fusion partner of mouse hybridomas. Stable hybrids were selected by culturing the fused cells on HAT medium with ouabain, which is toxic for both parental cells.

Immunostaining of LNA-1 2–72 h after fusion showed that the LNA-1 bodies were confined to the human nucleus in the heterokaryons during the whole period (Fig. 5A). The same phenomenon was observed in BCBL-1–Sp2-0 and BCBL-1–NIH3T3 heterokaryons (data not shown). Following the completion of a full cell cycle and fusion of the two nuclei, LNA-1 bodies were associated with the human chromatin and avoided the mouse chromatin (Fig. 5B).

Long term culturing led to the gradual loss of human chromosomes. Following the nearly complete loss of human chromosomes, LNA-1 persisted in the BC-1–Sp2-0 hybrids during 8 months of culturing, whereafter it started to disappear gradually. In contrast, the EBV-encoded EBNAs were com-

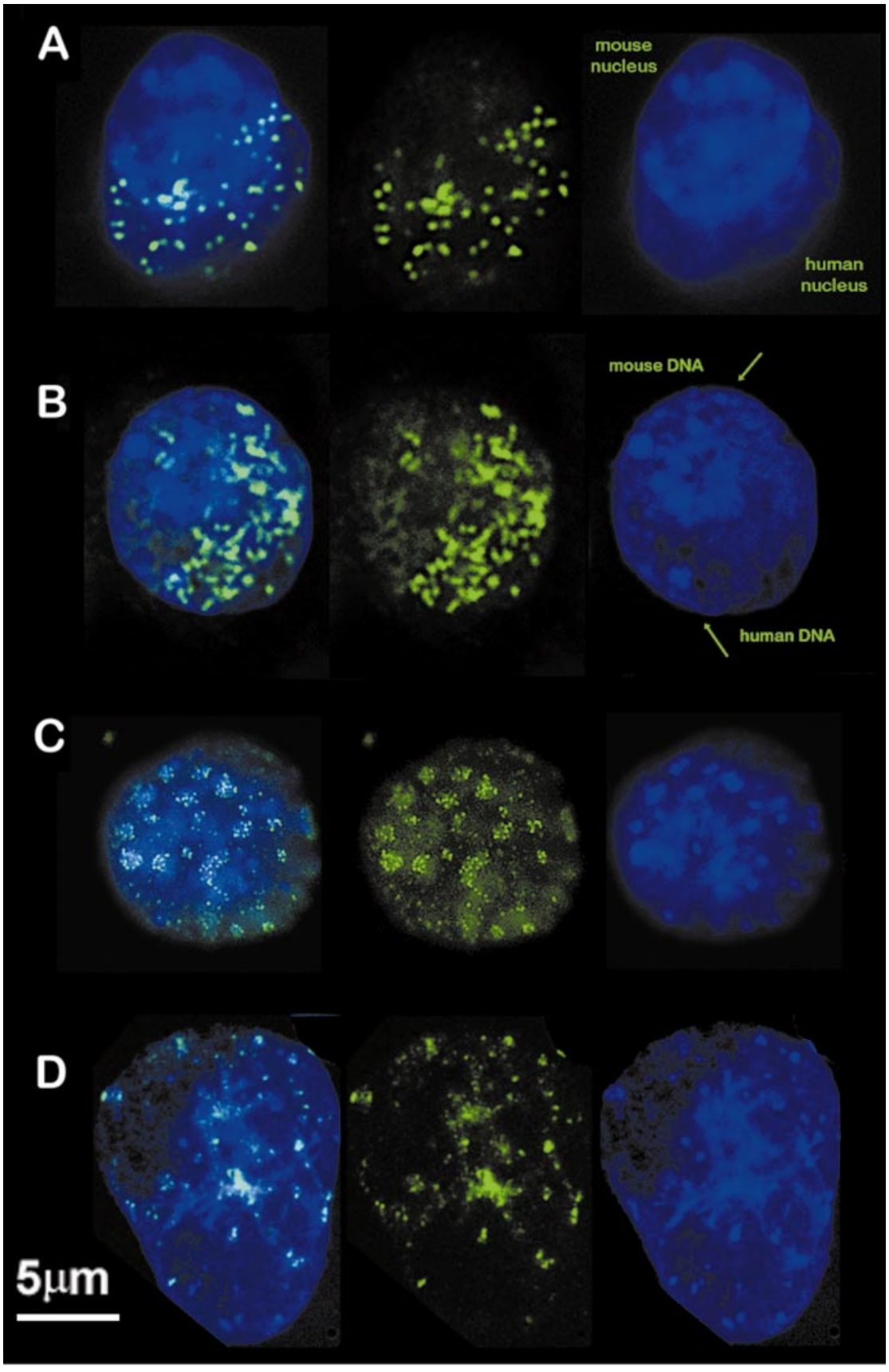
A
mouse
nucleus
human
nucleus
B
mouse DNA
human DNA
C
D
5μm

pletely lost from the hybrids by 2 weeks after the fusion. The presence of the HHV-8 genome and the absence of EBV DNA from the hybrids was also confirmed by PCR at the end of the third month (Fig. 4G).

Interestingly LNA-1 bodies were still present in the late hybrids after the loss of human chromosomes. They were associated with the murine pericentromeric heterochromatin (Fig. 5C).

Spreading the chromatin with the help of a rapidly expanding fluid drop generated extended nuclear sheets with sharp borders between euchromatin and heterochromatin. Immunostaining confirmed the close association between the LNA-1 bodies and mouse heterochromatin (Fig. 5D).

Association of LNA-1 with metaphase chromosomes

In dividing cells LNA-1 containing nuclear bodies remains attached to the chromosomes (Szekely *et al.*, 1998). The number of nuclear bodies varies greatly among individual metaphases (Fig. 6A). LNA-1 bodies appear often as symmetric doublets in both interphase and metaphase cells. The presence of these structures suggested that they might associate with both copies of a given sequence that could indicate sequence-specific DNA interaction. Analysis of metaphase cells showed, however, that the LNA-1 doublets were frequently located on only one side of one of the sister chromatids (Fig. 6B). This was also observed in metaphases where intact chromosomes were visualized by three-dimensional reconstitution from a series of optical sections.

LNA-1 remains also associated with the mouse chromosomes in long term BC-1–Sp2-0 hybrids. While LNA-1 forms mainly distinct bodies on human chromosomes, it often paints large areas of entire mouse chromosomes. Association with different chromosomes is very non-homogeneous. Within the same metaphase plate some chromosomes may be intensely stained while others are completely negative. No staining was detectable on the pericentromeric regions of the mouse chromosomes (Fig. 6C).

LNA-1 in apoptotic cells

Small numbers of apoptotic cells are present in almost all cell cultures. Apoptotic cells are easily recognized by Hoechst 33258 staining by the loss of nuclear structures followed by the condensation and eventual fragmentation of the nuclear remnants, leading to the formation of apoptotic bodies. In both BC-1 and BCBL-1 cells LNA-1 foci persisted even in advanced apoptotic cells but were not included in the apoptotic bodies (Fig. 6 D).

Nuclear distribution of LNA-1 and EBNAs in BCBL-1–LCL hybrids

Since LNA-1 is the major latency-associated nuclear protein of HHV-8, it might share functions with some of the six EBNAs encoded by EBV. We have previously shown that BC-1 cells that harbour both viruses show strict type I EBV latency (express only EBNA-1 and LMP2A). They were found to accumulate EBNA-1 and LNA-1 in distinct nuclear foci with no significant overlap (Szekely *et al.*, 1998).

In the present study we have extended these experiments to study the possible relationship between EBNA-2, -5, -6 and LNA-1 in cell hybrids between the EBV-negative BCBL-1 cells and the EBV-immortalized LCL IB-4, which expresses all six EBNAs. Double fluorescence staining of the heterokaryons for LNA-1 and the EBNAs at different time-points after the fusion showed that while EBNA-1, -2, -5, and -6 equilibrated between the nuclei within 40 h, LNA-1 remained associated with the original BCBL-1 nucleus during the entire observation time ($>$ 72 h). There was no co-localization between any of the EBNAs and LNA-1 in the double positive nuclei. Interestingly, the different EBNAs equilibrated between the nuclei of the heterokaryons with different kinetics. EBNA-5 was the most mobile, showing full equilibration by 4 h, whereas EBNA-6 needed more than 40 h (Table 1 and Fig. 7A–I). We also stained the EBV-encoded latent membrane protein LMP-1 together with LNA-1 and showed that it was distributed on the entire surface of the hybrids as early as 5 h after fusion (not shown). The staining intensity of EBNA-6 and LMP-1 but not EBNA-2 and EBNA-5 was reduced in the older (66 h) hybrids.

LNA-1 in freshly infected cells

We found that ECV, a spontaneously immortalized human endothelial cell line, and K562 erythroleukaemia cells can be infected with HHV-8 using supernatants of TPA-induced BCBL-1 cells. By 48 h 1–5% of the infected population became LNA-1-positive and persisted in the culture for at least 8 weeks but was overgrown later by LNA-1-negative cells. The LNA-1 staining pattern was mainly associated with high DNA density areas (Fig. 7 K).

GFP–LNA-1-C′ in transfected cells

The C-terminal part of LNA-1 harbours a putative nuclear translocation signal. We tested the surrounding 182 amino acid long region for subcellular localization by fusing the LNA-1 fragment to green fluorescent protein (GFP). Upon transfection into CV-1 cells the fusion protein accumulated in the nucleus. In most cells the protein showed a nearly homo-

Fig. 5. LNA-1 in BC-1–Sp2-0 human–mouse hybrids. (A) Heterokaryon 48 h after fusion. The murine nucleus can be identified by the pericentromeric heterochromatin blobs that are in contrast against the more homogeneous human nucleus. LNA-1 staining is confined to the human nucleus. (B) Synkaryon 5 days after fusion containing approximately equal amounts of murine and human DNA. LNA-1 remains predominantly in the human (pericentromeric heterochromatin-free, homogeneous) half of the nucleus. (C) Two months after fusion. Almost all human chromosomes are lost from the hybrid. LNA-1 is associated with the mouse heterochromatin. (D) Mechanical spreading of late hybrid nuclei confirms this association. DNA staining (right), LNA-1 staining (middle), superposition (left).

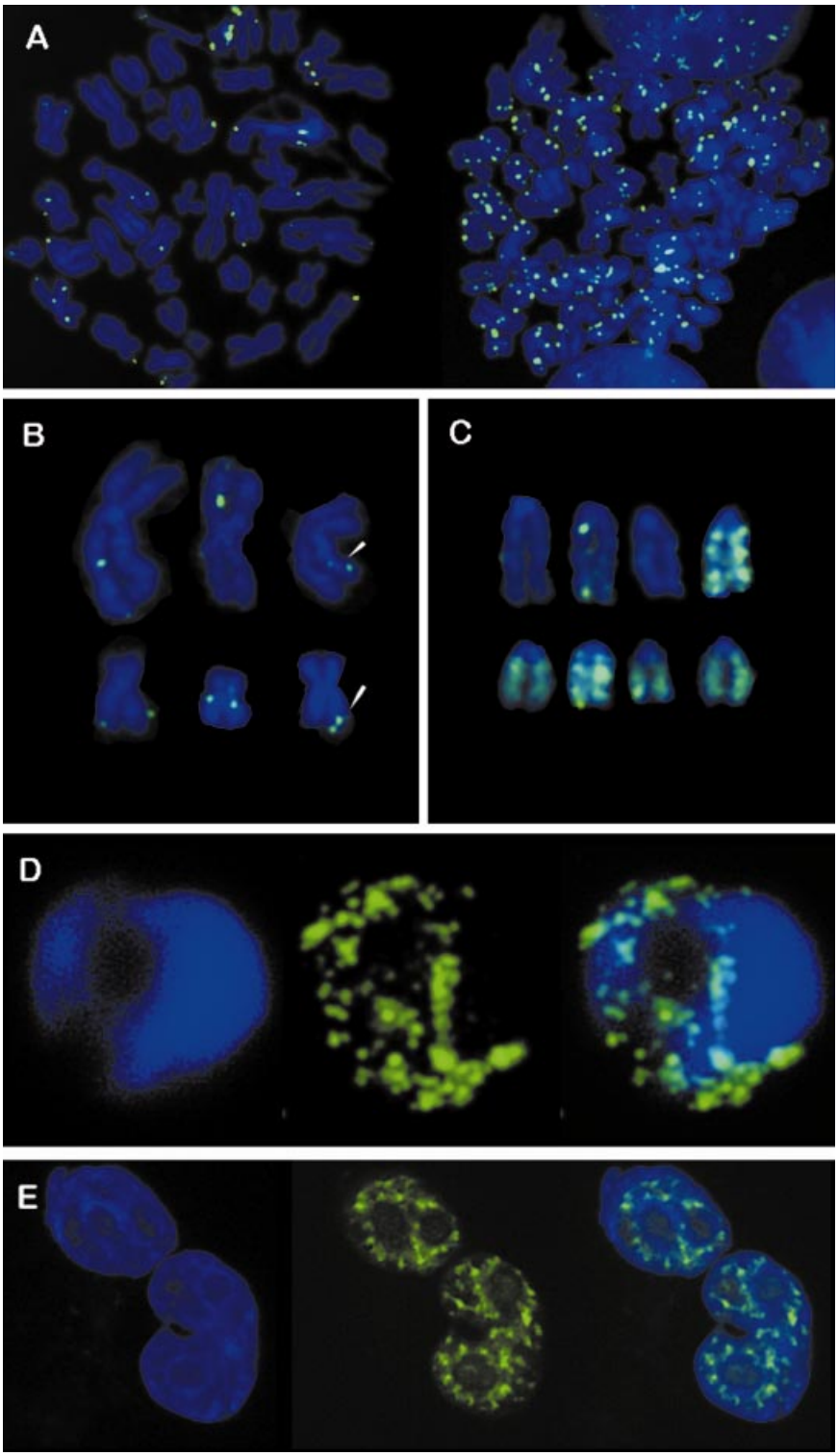

Fig. 6. Association of LNA-1 with mitotic chromosomes. (A) The number of LNA-1 bodies varies greatly from metaphase to metaphase within the same cell population. (B) LNA-1 bodies associate with human chromosomes as solitary foci, doublets on the two sister chromatids, or doublets on the same sister chromatid (arrowheads). (C) Mouse chromosomes from a metaphase of a 6 month old BC-1–Sp2-0 hybrid. LNA-1 can form solitary blobs, aggregates or paint entire chromosome arms homogeneously. The pericentromeric region is spared, as a rule. (D) LNA-1 bodies persist in apoptotic cells but get separated from the condensed nuclear remnants. (E) The C-terminal fragment of LNA-1 (aa 939–1121) is sufficient to induce nuclear accumulation of the GFP fusion protein in CV-1 cells. The fusion protein does not associate with the heterochromatin, however, but remains in the low DNA density areas.

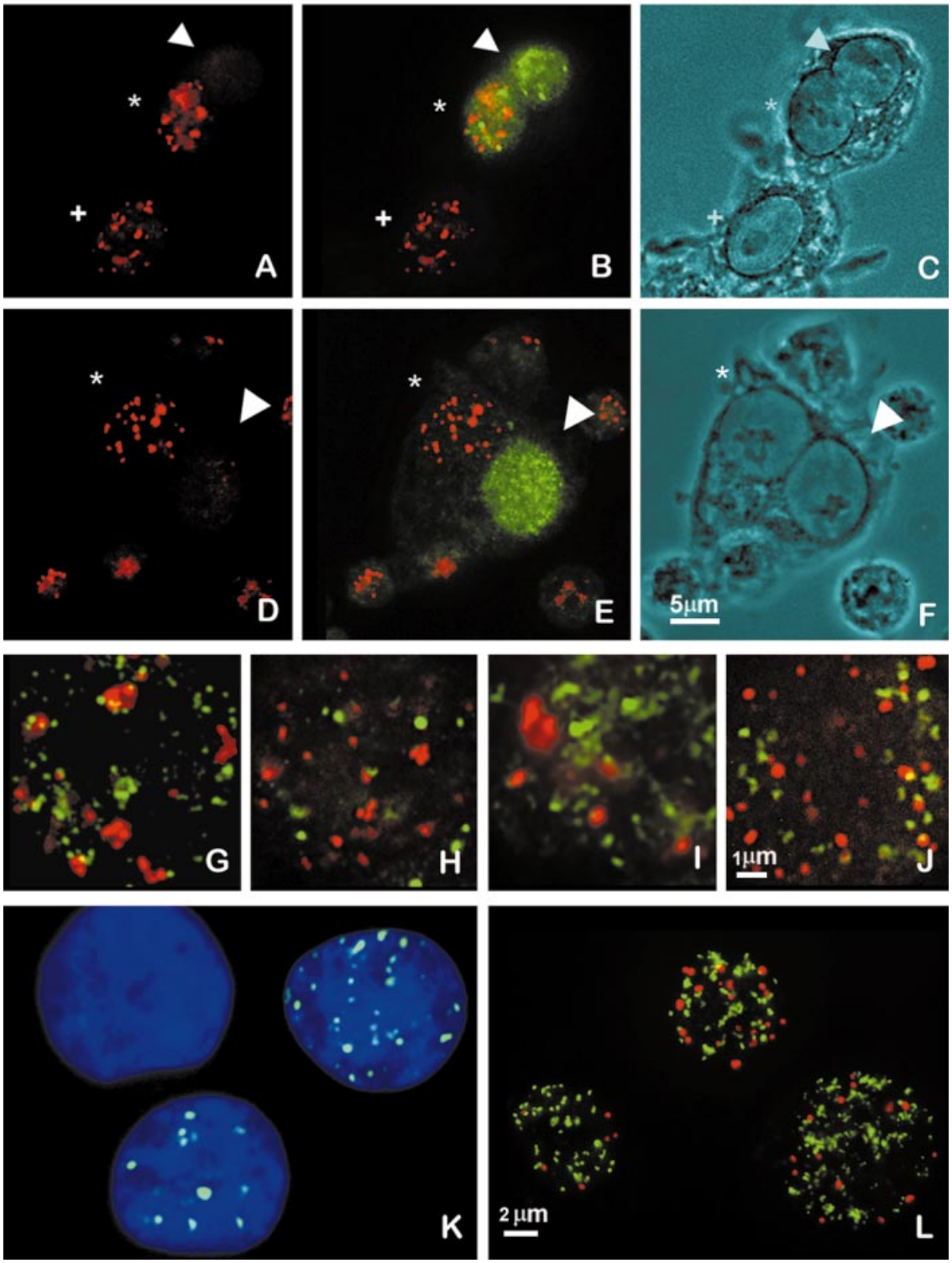

Fig. 7. LNA-1 stays in the BCBL-1 nucleus in BCBL-1$^{(HHV\text{-}8+/EBV-)}$–IB4$^{(HHV\text{-}8-/EBV+)}$ heterokaryons, whereas the EBNAs equilibrate between the two nuclei. EBNA-5 equilibrates most rapidly (< 4 h), whereas the slowest, EBNA-6, needs ≈ 40 h. (A) LNA-1 staining of a heterokaryon and a non-fused BCBL-1 cell (+) 5 h after the fusion. (B) LNA-1 (red) and EBNA-5 (green) in superposition; (C) phase contrast. In the heterokaryon the BCBL-1 nucleus (*) retains LNA-1 staining and also accumulates EBNA-5. The partner nucleus from IB4 (▲) retains EBNA-5 staining but remains negative for LNA-1. (D)–(F) A heterokaryon 26 h after the fusion double-stained for LNA-1 (red) and EBNA-6 (green). (D) LNA-1 staining alone, (E) superimposed EBNA-6 staining, (F) phase contrast. No equilibration is detectable yet. IB4 nucleus (▲), BCBL-1 nucleus (*). (G)–(I) Double staining of LNA-1 (red) and EBNA-2 (G), EBNA-5 (H) and EBNA-6 (I) (all green) in heterokaryon nuclei of

Table 1. Migration of EBNAs and LNA-1 to the partner nucleus in heterokaryons between BCBL-1 (HHV-8$^+$/EBV$^-$) and IB4 (HHV-8$^-$/EBV$^+$) cells

	Time post-fusion (h)					
	4	5	17	26	41	66
EBNA-5	+	+	+	+	+	+
EBNA-2	ND	−	+	+	+	+
EBNA-1	ND	−	ND	+	+	ND
EBNA-6	ND	−	−	−	+	+
LNA-1	−	−	−	−	−	−

geneous nuclear distribution, but occasionally accumulated in distinct foci. However, these foci primarily localized to the euchromatin (Fig. 6E).

Relationship between LNA-1 and ND10 bodies

The ND10 bodies (Daniel *et al*., 1993) are nuclear structures that are frequently targeted by viral regulatory proteins. Their components, PML and Sp100 proteins, are induced by interferon alfa and gamma. Double fluorescence staining of LNA-1 and either PML or Sp100 showed that the LNA-1 bodies and ND10 occupy different nuclear domains. (Fig. 7L and J respectively).

Discussion

The cell nucleus is highly structured and contains several different compartments (Lamond *et al*., 1998). In addition to the chromatin, it harbours the nucleoli, splicing islands and a fast expanding flora of nuclear bodies, exemplified by coiled bodies, ND10 (PML), as well as replication and transcription foci (Jackson, 1997).

The degree of chromatin condensation affects gene expression. Nuclear areas with highly condensed DNA are transcriptionally inactive, as a rule (Wallrath, 1998). Chromatin condensation is regulated in several ways, such as methylation of CpG sites, acetylation of core histones or association of protein complexes such as the Polycomb group proteins (Jenuwein *et al*., 1998; Saurin *et al*., 1998; Turner, 1998). The latter form distinct bodies that associate with heterochromatin during the interphase and remain associated with the chromosomes during cell division.

We have found that LNA-1-containing nuclear foci associate with the border of highly condensed chromatin. These foci are primarily bound to DNA but not to the nuclear matrix. No RNA is needed to maintain their structural integrity. Their number, size and morphology varies from cell to cell in established cell lines. This heterogeneity is also present in metaphase cells, indicating that it is not cell-cycle-dependent.

The association with the heterochromatin border is not restricted to BC cells but is also detectable in freshly infected erythroleukaemia and endothelial cells.

Binding of LNA-1 bodies to murine pericentromeric heterochromatin blobs in the nuclei of the BC-1–Sp2-0 hybrids but not to the pericentromeric regions of the murine metaphase chromosomes suggests that LNA-1 has a specific affinity to the *interphase* heterochromatin but not to specific sequences of the pericentromeric region. This is consistent with the random association of LNA-1 with human metaphase chromosomes. The persistent association of LNA-1 with the human chromatin in the mouse–human hybrids and its failure to equilibrate with the partner nucleus in both human–human and human–mouse heterokaryons suggests that LNA-1 has a high affinity to certain low turnover structures on the heterochromatin of the donor nuclei.

The recent demonstration of co-localization between LNA-1 foci and the HHV-8 DNA suggests that these low turnover structures are the viral genomes themselves (Ballestas *et al*., 1999).

LNA-1 has a very unusual primary structure. It contains a highly hydrophilic central domain of multiple repeats of glutamate, glutamine and asparagine, flanked by proline-rich N-terminal and basic C-terminal domains. The latter also harbours a putative nuclear translocation signal that we found capable of accumulating in the nucleus in the absence of other domains.

The peculiar distribution of LNA-1 might suggest that it participates in the control of euchromatin/heterochromatin transition. Upon docking to the border of the heterochromatin, the strongly acidic middle domain might facilitate the opening of closed heterochromatic areas in a similar way as the histone acetylation-induced charge shift opens up condensed chromatin.

The LNA-1 foci are clearly different from the ND10 bodies that are frequent targets of viral regulatory proteins (Maul, 1998). LNA-1 does not co-localize with the ND10 components PML and Sp100. Unlike ND10, the LNA-1 bodies do not resist mechanical spreading and stay on the mitotic chromosomes. High resolution three-dimensional reconstitution of LNA-1 clusters also suggest that unlike the ND10s the LNA-1 bodies do not have rigid borders but tend to fill up spaces excluded

BCBL-1 origin 41 h after the fusion. No co-localization is detectable. (J) and (L), LNA-1 (red) does not co-localize with ND10 bodies as shown by double staining for Sp100 (J) or PML (L) (both green) in BCBL-1 nuclei. The separate localization is maintained independently of the morphological variations of LNA-1 staining (L). (K) LNA-1 bodies in freshly HHV-8-infected ECV nuclei show a similar distribution as in BC cells.

from other structures. These spaces often communicate with each other.

Since LNA-1 is the major latency-associated nuclear antigen of HHV-8, it has been suggested that it may have a similar function to some of the EBV-encoded EBNAs. No co-localization was detectable between LNA-1 and EBNA-1, -2, -5 and -6 in the BC–LCL heterokaryons.

This work was supported by Cancerfonden, Sweden and CRI/Concern Foundation USA.

References

Ballestas, M. E., Chatis, P. A. & Kaye, K. M. (1999). Efficient persistence of extrachromosomal KSHV DNA mediated by latency-associated nuclear antigen. *Science* **284**, 641–644.

Boshoff, C. & Weiss, R. A. (1998). Kaposi's sarcoma-associated herpesvirus. *Advances in Cancer Research* **75**, 57–86.

Daniel, M. T., Koken, M., Romagne, O., Barbey, S., Bazarbachi, A., Stadler, M., Guillemin, M. C., Degos, L., Chomienne, C. & de The, H. (1993). PML protein expression in hematopoietic and acute promyelocytic leukemia cells. *Blood* **82**, 1858–1867.

Dittmer, D., Lagunoff, M., Renne, R., Staskus, K., Haase, A. & Ganem, D. (1998). A cluster of latently expressed genes in Kaposi's sarcoma-associated herpesvirus. *Journal of Virology* **72**, 8309–8315.

Flore, O., Rafii, S., Ely, S., O'Leary, J. J., Hyjek, E. M. & Cesarman, E. (1998). Transformation of primary human endothelial cells by Kaposi's sarcoma-associated herpesvirus. *Nature* **394**, 588–592.

He, J., Bhat, G., Kankasa, C., Chintu, C., Mitchell, C., Duan, W. & Wood, C. (1998). Seroprevalence of human herpesvirus 8 among Zambian women of childbearing age without Kaposi's sarcoma (KS) and mother–child pairs with KS. *Journal of Infectious Diseases* **178**, 1787–1790.

Holmvall, P. & Szekely, L. (1999). Computer programs that allow fast acquisition, visualization and overlap quantitation of fluorescent 3D microscopic objects using nearest neighbor deconvolution algorithm. *Applied Immunochemistry & Molecular Morphology* (in press).

Jackson, D. A. (1997). Chromatin domains and nuclear compartments: establishing sites of gene expression in eukaryotic nuclei. *Molecular Biology Reports* **24**, 209–220.

Jenuwein, T., Laible, G., Dorn, R. & Reuter, G. (1998). SET domain proteins modulate chromatin domains in eu- and heterochromatin. *Cellular and Molecular Life Sciences* **54**, 80–93.

Kedes, D. H., Lagunoff, M., Renne, R. & Ganem, D. (1997). Identification of the gene encoding the major latency-associated nuclear antigen of the Kaposi's sarcoma-associated herpesvirus. *Journal of Clinical Investigation* **100**, 2606–2610.

Kennedy, M. M., Cooper, K., Howells, D. D., Picton, S., Biddolph, S., Lucas, S. B., McGee, J. O. & O'Leary, J. J. (1998). Identification of HHV8 in early Kaposi's sarcoma: implications for Kaposi's sarcoma pathogenesis. *Molecular Pathology* **51**, 14–20.

Kliche, S., Kremmer, E., Hammerschmidt, W., Koszinowski, U. & Haas, J. (1998). Persistent infection of Epstein–Barr virus-positive B lymphocytes by human herpesvirus 8. *Journal of Virology* **72**, 8143–8149.

Knowles, D. M. & Cesarman, E. (1997). The Kaposi's sarcoma-associated herpesvirus (human herpesvirus-8) in Kaposi's sarcoma, malignant lymphoma, and other diseases. *Annals of Oncology* **8**, 123–129.

Lamond, A. I. & Earnshaw, W. C. (1998). Structure and function in the nucleus. *Science* **280**, 547–553.

Martin, J. N., Ganem, D. E., Osmond, D. H., Page-Shafer, K. A., Macrae, D. & Kedes, D. H. (1998). Sexual transmission and the natural history of human herpesvirus 8 infection. *New England Journal of Medicine* **338**, 948–954.

Maul, G. G. (1998). Nuclear domain 10, the site of DNA virus transcription and replication. *Bioessays* **20**, 660–667.

Mayama, S., Cuevas, L. E., Sheldon, J., Omar, O. H., Smith, D. H., Okong, P., Silvel, B., Hart, C. A. & Schulz, T. F. (1998). Prevalence and transmission of Kaposi's sarcoma-associated herpesvirus (human herpesvirus 8) in Ugandan children and adolescents. *International Journal of Cancer* **77**, 817–820.

Moore, P. S. & Chang, Y. (1998). Antiviral activity of tumor-suppressor pathways: clues from molecular piracy by KSHV. *Trends in Genetics* **14**, 144–150.

Neipel, F., Albrecht, J. C. & Fleckenstein, B. (1998). Human herpesvirus 8 – the first human Rhadinovirus. *Journal of the National Cancer Institute Monographs* **23**, 73–77.

Nicholas, J., Zong, J. C., Alcendor, D. J., Ciufo, D. M., Poole, L. J., Sarisky, R. T., Chiou, C. J., Zhang, X., Wan, X., Guo, H. G., Reitz, M. S. & Hayward, G. S. (1998). Novel organizational features, captured cellular genes, and strain variability within the genome of KSHV/HHV8. *Journal of the National Cancer Institute Monographs* **23**, 79–88.

Pokrovskaja, K., Trivedi, P., Klein, G. & Szekely, L. (1997). Epstein–Barr virus-encoded LMP1 protein upregulates the pNDCF group of nucleoskeleton–cytoskeleton-associated proteins. *Journal of General Virology* **78**, 2031–2040.

Rabkin, C. S., Schulz, T. F., Whitby, D., Lennette, E. T., Magpantay, L. I., Chatlynne, L. & Biggar, R. J. (1998). Interassay correlation of human herpesvirus 8 serologic tests. HHV-8 Interlaboratory Collaborative Group. *Journal of Infectious Diseases* **178**, 304–309.

Rainbow, L., Platt, G. M., Simpson, G. R., Sarid, R., Gao, S. J., Stoiber, H., Herrington, C. S., Moore, P. S. & Schulz, T. F. (1997). The 222- to 234-kilodalton latent nuclear protein (LNA) of Kaposi's sarcoma-associated herpesvirus (human herpesvirus 8) is encoded by orf73 and is a component of the latency-associated nuclear antigen. *Journal of Virology* **71**, 5915–5921.

Sarid, R., Flore, O., Bohenzky, R. A., Chang, Y. & Moore, P. S. (1998). Transcription mapping of the Kaposi's sarcoma-associated herpesvirus (human herpesvirus 8) genome in a body cavity-based lymphoma cell line (BC-1). *Journal of Virology* **72**, 1005–1012.

Saurin, A. J., Shiels, C., Williamson, J., Satijn, D. P., Otte, A. P., Sheer, D. & Freemont, P. S. (1998). The human polycomb group complex associates with pericentromeric heterochromatin to form a novel nuclear domain. *Journal of Cell Biology* **142**, 887–898.

Szekely, L., Jiang, W.-Q., Pokrovskaja, K., Wiman, K. G., Klein, G. & Ringertz, N. (1995). Reversible nucleolar translocation of Epstein–Barr virus-encoded EBNA-5 and hsp70 proteins after exposure to heat shock or cell density congestion. *Journal of General Virology* **76**, 2423–2432.

Szekely, L., Pokrovskaja, K., Jiang, W. Q., de The, H., Ringertz, N. & Klein, G. (1996). The Epstein–Barr virus-encoded nuclear antigen EBNA-5 accumulates in PML-containing bodies. *Journal of Virology* **70**, 2562–2568.

Szekely, L., Chen, F., Teramoto, N., Ehlin-Henriksson, B., Pokrovskaja, K., Szeles, A., Manneborg-Sandlund, A., Löwbeer, M., Lennette, E. T. & Klein, G. (1998). Restricted expression of Epstein–Barr virus (EBV)-encoded, growth transformation-associated antigens in an EBV- and human herpesvirus type 8-carrying body cavity lymphoma line. *Journal of General Virology* **79**, 1445–1452.

Turner, B. M. (1998). Histone acetylation as an epigenetic determinant of long-term transcriptional competence. *Cellular and Molecular Life Sciences* **54**, 21–31.

Wallrath, L. L. (1998). Unfolding the mysteries of heterochromatin. [Review, 66 refs]. *Current Opinion in Genetics and Development* **8**, 147–153.

Weiss, R. A., Whitby, D., Talbot, S., Kellam, P. & Boshoff, C. (1998). Human herpesvirus type 8 and Kaposi's sarcoma. *Journal of the National Cancer Institute Monographs* **23**, 51–54.

Whitby, D. & Boshoff, C. (1998). Kaposi's sarcoma herpesvirus as a new paradigm for virus-induced oncogenesis. *Current Opinion in Oncology* **10**, 405–412.

Zong, J. C., Metroka, C., Reitz, M. S., Nicholas, J. & Hayward, G. S. (1997). Strain variability among Kaposi sarcoma-associated herpesvirus (human herpesvirus 8) genomes: evidence that a large cohort of United States AIDS patients may have been infected by a single common isolate. *Journal of Virology* **71**, 2505–2511.

Received 21 May 1999; Accepted 9 July 1999